

Dynamical symmetry of chaotic systems

Li Junqing

China Center of Advanced Science and Technology (World Laboratory) P.O. Box 8730, Beijing 100080, People's Republic of China and Institute of Modern Physics, Academia Sinica, Lanzhou 730000, People's Republic of China

Zhu Jieding

Department of Modern Physics, Lanzhou University, Lanzhou 730001, People's Republic of China

Gu Jinnan

Institute of Modern Physics, Academia Sinica, Lanzhou 730000, People's Republic of China

(Received 17 May 1993; revised manuscript received 6 January 1995)

The spectral fluctuation properties of a quantum system are related closely to the dynamical symmetries of the system. The equipotential lines of the system intuitively give information about the symmetry of the system, indicating the degree of symmetry breaking as well as how symmetry is lost. Chaotic motion appears when the curvature of the equipotential lines becomes negative. The energy spectrum of a helium atom is calculated, and by analyzing spectral fluctuations, it is found that the electron-electron interaction is not sufficient to change the integrable dynamical behavior of the two electrons in the central field of a nucleus. Even when this interaction is artificially amplified to the greatest possible extent below the dissociation limit, the Kolmogorov-Arnold-Moser theorem still qualitatively governs the quantum system. This coincides with the indication of the curvature of the equipotential lines that we discussed in this paper.

I. INTRODUCTION

The classical chaotic behavior of nonlinear dynamical systems has exhibited intriguing phenomena which are connected with the destruction of at least one integral of the motion. By analogy with classical chaos, in the search for quantum chaos it is natural to focus attention on systems with manifestations of broken dynamical symmetry. A dramatic phenomenon was shown by Bohigas *et al.*,¹ in which it is described that during the transition of a classical analog of a quantum system from regular to chaotic motion, the quantum behavior does not manifest itself in a specific energy level or quantum state, but in the statistical fluctuation properties of the global energy levels of the system. The system whose classical analog is integrable shows Poisson fluctuations whereas the systems whose classical analogues are fully chaotic show Gaussian-orthogonal-ensemble (GOE) fluctuation patterns.² Since both Poisson and GOE distribution functions contain no free parameters, Bohigas *et al.* conjectured that this phenomenon was generic. A famous example is the two-dimensional billiard. A billiard consists in the motion of a free-point particle of mass m in a domain Γ of the plane of arbitrary shape. The particle is elastically reflected when it hits the boundary of Γ , according to the laws of specular reflection. The circular billiard is integrable whereas Sinai's and Bunimovich's stadium billiards are chaotic, since the latter two cases do not conserve angular momentum.² When treating the problem as a quantum system one has to solve the Schrödinger equation

$$(-\hbar^2/2m)\nabla^2\psi_n(\vec{r}) = E_n\psi_n(\vec{r})$$

with the vanishing of the wave function $\psi_n(\vec{r})$ at the boundary Γ . A particle is moving in a potential well of infinite depth, and the shape of the equipotential surface of each case is the same figure as the type of billiards. Their energy spectra exactly show a Poisson fluctuation pattern for a classically integrable system, and a GOE pattern for a classically chaotic system.

The hydrogen atom is a system possessing an abundance of symmetry. The rotational invariance of the system is destroyed when a hydrogen atom is in a uniform magnetic field, so that the transition of the motion from regular to chaotic behavior can be observed, if the magnetic field is strong enough. A helium atom has an extra electron, and the interaction between two electrons has also changed the spatial uniformity. Its spectral fluctuation properties are calculated in the present work, but a substantial deviation from the Poisson fluctuation pattern is not found. By analyzing the characteristics of the spectral fluctuation properties of different systems such as the helium atom and hydrogen atom in a uniform magnetic field and other systems, some interesting phenomena are observed: for some systems, their spectra have a globally consistent fluctuation pattern, i.e., any part of the spectrum shows the same fluctuation properties as those of the whole spectrum. For some other systems the highly excited part of the spectrum may show different fluctuation patterns than that of the low-lying part of the spectrum. There may exist a boundary in the spectrum, which divides the spectrum into two parts, the subspectrum above the boundary and the other one below the boundary showing different fluctuation properties. Or the energy levels may have to be rescaled in some way in order to have a globally consistent mea-

surement for the fluctuation property.⁴ Inspired by the different behaviors of billiards with different boundaries, we have noticed that the shapes of equipotential lines for each individual system, as well as the distributions of the equipotential lines, do offer some information about symmetry breaking and the dynamical behaviors of the systems. And since the evaluation of the equipotential lines meets no new obstacles by increasing the number of system dimensions, it is possible to overcome the multi-dimensional complexity, and to approach the substantial physics which is of interest directly.

In Sec. II the dynamical behavior of three example systems are qualitatively described. In each of them at least one of the good quantum numbers is destroyed, and with increasing disturbance their energy spectra show different statistical fluctuation properties because their equipotential lines deform in different ways. In Sec. III the stability of dynamics and the curvature of the potential are analyzed. The condition of negative curvature appearance for the given examples is evaluated, and agreement with dynamical calculations is found. Finally the conclusions are given in Sec. IV.

II. THE SHAPE OF EQUIPOTENTIAL LINES AND THE CHARACTERISTICS OF DYNAMICAL MOTION

In the following we study three examples. In all examples at least one good quantum number is destroyed, but their energy spectra show different fluctuation behavior: With increasing strength of turbulence, for system A always only a part of the highly excited energy spectrum shows GOE fluctuation; for system B the energy spectrum transforms from Poisson to GOE pattern as a whole; for system C the energy spectrum always shows Poisson pattern.

A. A hydrogen atom in a magnetic field

The problem of a hydrogen atom in a magnetic field has been intensively studied.^{3,4} The Hamiltonian for a hydrogen atom is

$$H = p^2/2 - 1/r \quad (2.1)$$

in atomic units with the number of good quantum numbers and degrees of freedom being equal. The potential is spherically symmetric. The energy spectrum of the system shows Poisson fluctuations. The Hamiltonian of the atom in a magnetic field is

$$H = \frac{p^2}{2} - \frac{1}{r} + \frac{\gamma}{2} L_z + \frac{\gamma^2}{8} (x^2 + y^2), \quad (2.2)$$

where $\gamma = B/B_c$ is the reduced magnetic field ($B_c = 2.35 \times 10^5 T$). Now the angular momentum l is no longer a good quantum number. Only its projection m remains a good quantum number. Correspondingly the equipotential lines in the x - y plane are still concentric circles,

while in the z - x and z - y planes they are stretched irregularly to different extents. In Fig. 1 the equipotential lines are illustrated for $L_z = 0$. It is shown that for the deep part of the potential, i.e., the lower excitation region, the rotational invariance remains and the equipotential lines are still circles. With increasing excitation energy the equipotential line begins to deform, and the higher the excitation energy is, the more the equipotential line becomes stretched. Using Friedrich's⁴ scaled coordinate and momenta

$$\tilde{r} = \gamma^{2/3} \vec{r}, \quad \tilde{p} = \gamma^{-1/3} \vec{p}, \quad (2.3)$$

in cylindrical coordinates the Hamiltonian of Eq. (2.2) can be scaled and written as

$$\gamma^{-2/3} H = \tilde{H} = \frac{1}{2} \tilde{P}_\rho^2 + \frac{1}{2} \tilde{P}_z^2 + \frac{\tilde{L}_z^2}{2\tilde{\rho}^2} + \frac{1}{8} \tilde{\rho}^2 - (\tilde{\rho}^2 + z^2)^{-1/2}. \quad (2.4)$$

This equation shows that the classical dynamics only depends on the scaled energy ϵ defined by

$$\epsilon \equiv E\gamma^{-3/2}. \quad (2.5)$$

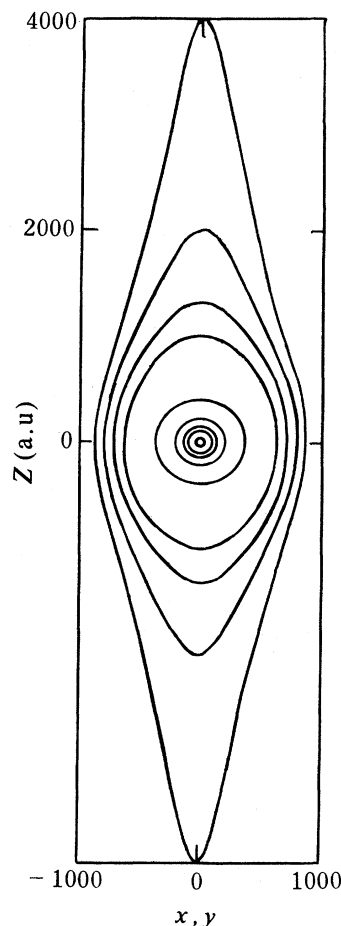


FIG. 1. The equipotential lines in the $(x$ - z or y - z) plane for a hydrogen atom in a uniform magnetic field.

This means that for the same scaled energy ϵ the shape of the equipotential lines for the system should be similar. For a very strong magnetic field the dynamical behavior could still be regular if the energy of the electron is very low. On the contrary, in a very weak magnetic field the dynamical behavior could be chaotic if the excitation energy is high, indicating the extreme importance of the determination of the scaled energy. Looking back to the two-dimensional classical and quantum billiards, it is not so abrupt to compare the shape of the equipotential lines with the boundary shape for the billiards. In Fig. 2 the Poincare sections are shown for two-dimensional billiards with the boundaries determined by the equipotential lines for a hydrogen atom in a magnetic field for the scaled energy $\epsilon = -0.54$ (upper part) and $\epsilon = -0.12$ (below), respectively. The equation of the equipotential lines is as $\epsilon \equiv \frac{1}{8}\tilde{\rho}^2 - (\tilde{\rho}^2 + z^2)^{-1/2}$ with $\tilde{L}_z=0$. The motions of billiards show a regular pattern for the case of

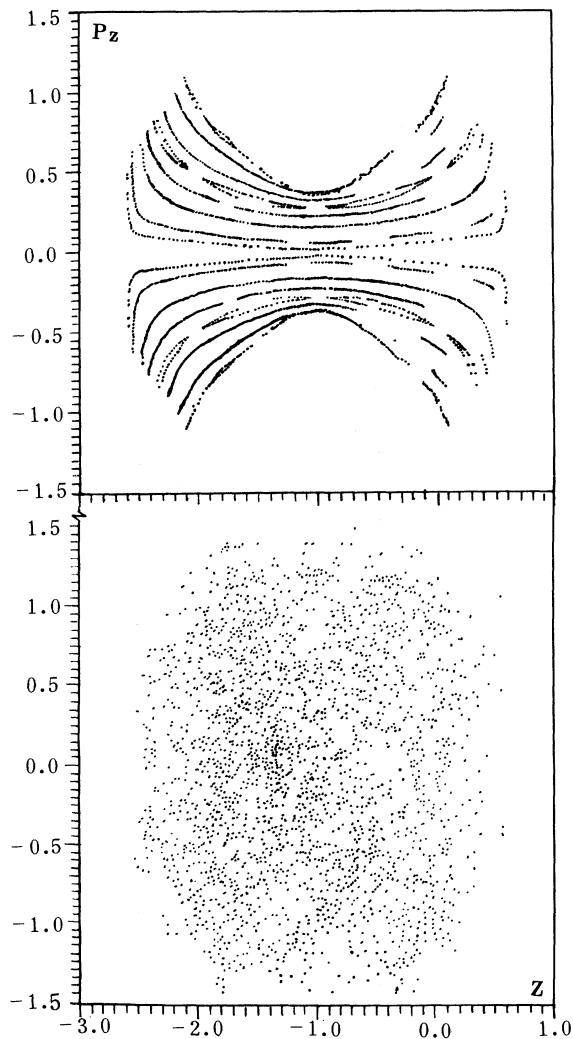


FIG. 2. Poincaré surfaces of section for a two-dimensional billiard with the boundaries determined by equipotential lines of the hydrogen atom in a magnetic field: above for $\epsilon = -0.54$ and below $\epsilon = -0.12$.

$\epsilon = -0.54$ and chaotic motion for $\epsilon = -0.12$. Friedrich and Wintgen's⁴ results from dynamical calculations in a three-dimensional potential energy for these two cases are consistent with the conclusion. So the characteristic breaking of the dynamical symmetry of the system is prominently characterized by the geometrical symmetry of the system. The chaotic behavior demands a certain deformation of the equipotential lines of the system, which characterizes the strength of the turbulence demanded by the Kolmogorov-Arnold-Moser (KAM) theorem. The specific quantitative evaluation of the deformation needed for the transition of the dynamical motion from regular to chaotic type will be given in Sec. III.

B. A system with energy scale invariance

For systems with scale invariance, the chaotic volume and the Lyapunov exponent are energy independent.⁷ The equipotential lines of the system show different patterns. In Fig. 3 the equipotential lines are shown for three-dimensional nonlinear oscillator with a Hamiltonian of the form

$$H = \frac{1}{2}(P_x^2 + P_y^2 + P_z^2) + x^4 + \frac{1}{2}y^4 + 2z^4 + ky^2(x^2 + z^2). \quad (2.6)$$

In the case of $k=10$, $z=0$ the dynamics show chaotic behavior.⁷ Although the distribution area confined by the equipotential lines is varying with increasing energy, the shapes of them remain similar. The degree of the dynamical symmetry breaking depends only on the parameter k and is independent of the potential energy. The potential formalism in Eq. (2.6) is, in principle, similar to that of Seligman, Verbaarschot, and Zirnbauer.^{5,6} They have checked whether the fluctuation measures are stationary for each part of the spectrum within the spectrum span considered, and the conclusion is positive. It

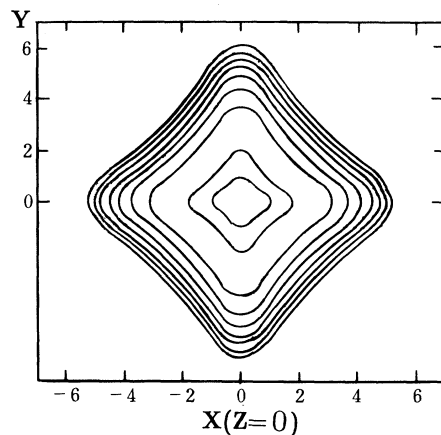


FIG. 3. The equipotential lines for the potential in Eq. (2.6) at $z=0$, $k=10$.

will be proved later that as long as the shapes of the equipotential lines for different energies remain similar, the spectral properties of the system do not vary with energy. Thus there is no boundary effect. The symmetrical property of the equipotential lines wonderfully and intuitively reflects the fluctuation character.

C. Spectral statistical fluctuation properties of a helium atom

Added to the nuclear central field, the electron-electron interaction destroys the single-electron rotational symmetry of a helium atom.

1. Calculation of the energy spectrum of a helium atom

The helium atom is a three-body problem and it has no precise solution. In a representation in Hilbert space with fixed angular momentum and fixed parity we have given an analytical formula to calculate both the matrix elements of the Hamiltonian and the corresponding selection rules. The truncation of the invariant space, in principle, depends on the precision needed.

The wave function in Hilbert space for a particular total angular momentum $\vec{J} = \vec{L} + \vec{S}$ can be written as

$$\begin{aligned} \Phi_{n_1, l_1, n_2, l_2}^{JMLS}(\vec{r}_1, \vec{r}_2) = & \frac{1}{\sqrt{2}} \left\{ \sum_{m_L, m_S} \langle L m_L S m_S | J M \rangle \sum_{m_1, m_2} \langle l_1 m_1 l_2 m_2 | L m_L \rangle \right. \\ & \sum_{m_{s_1}, m_{s_2}} \left\langle \frac{1}{2} m_{s_1} \frac{1}{2} m_{s_2} | s m_s \right\rangle [\phi_{n_1 l_1 m_1}(\vec{r}_1) \phi_{n_2 l_2 m_2}(\vec{r}_2) \\ & \left. - (-1)^{l_1 + l_2 - L} \phi_{n_2 l_2 m_2}(\vec{r}_1) \phi_{n_1 l_1 m_1}(\vec{r}_2) \right] \chi_{\frac{1}{2} m_{s_1}}(1) \chi_{\frac{1}{2} m_{s_2}}(2) \Big\}, \end{aligned} \quad (2.7)$$

where the $\phi_{nlm}(\vec{r})$ are hydrogen-type atom wave functions and $\chi_{\frac{1}{2} m_s}$ are the spin-wave functions with spin $\frac{1}{2}$ and spin projection m_s .

The wave function of the helium atom in the space of the $\Phi_{n_1, l_1, n_2, l_2}^{JMLS}$ of Eq. (2.7) is

$$\Psi^{JM}(\vec{r}_1, \vec{r}_2) = \sum_{n_1, l_1, n_2, l_2} C_{n_1 l_1 n_2 l_2 LS}^{JM} \Phi_{n_1 l_1 n_2 l_2}^{JMLS}(\vec{r}_1, \vec{r}_2), \quad (2.8)$$

which is the solution of the Hamiltonian

$$H = -\nabla_1^2/2 - 2/r_1 - \nabla_2^2/2 - 2/r_2 + 1/r_{12}. \quad (2.9)$$

Define

$$\left\langle \bar{1}, \bar{2} \left| \frac{1}{r_{12}} \right| 1, 2 \right\rangle \equiv \int \phi_{n_1' l_1' m_1'}(\vec{r}_1) \phi_{n_2' l_2' m_2'}(\vec{r}_2) \frac{1}{r_{12}} \phi_{n_1 l_1 m_1}(\vec{r}_1) \phi_{n_2 l_2 m_2}(\vec{r}_2) d\vec{r}_1 d\vec{r}_2$$

and

$$\left\langle \bar{2}, \bar{1} \left| \frac{1}{r_{12}} \right| 2, 1 \right\rangle \equiv \int \phi_{n_2' l_2' m_2'}(\vec{r}_1) \phi_{n_1' l_1' m_1'}(\vec{r}_2) \frac{1}{r_{12}} \phi_{n_2 l_2 m_2}(\vec{r}_1) \phi_{n_1 l_1 m_1}(\vec{r}_2) d\vec{r}_1 d\vec{r}_2, \quad (2.10)$$

with

$$l_1 + l_2 - L = \bar{l}, l_1' + l_2' - L' = \bar{l}'.$$

Then the secular equation becomes

$$\begin{aligned} & C_{n_1' l_1' n_2' l_2'}^{JM} (E_{01} + E_{02} - E) + \frac{1}{2} \sum_{n_1' l_1' n_2' l_2' LS} C_{n_1' l_1' n_2' l_2' LS}^{JM} \sum_{m_L m_S m_L' m_1 m_2 m_1' m_2'} \\ & \times (-1)^{-L - m_L - L' - m_L' - l_1 + l_2 - l_1' + l_2'} (2J + 1)(2L + 1)^{1/2} (2L' + 1)^{1/2} \\ & \times \begin{pmatrix} L & S & J \\ m_L & m_S & -M \end{pmatrix} \begin{pmatrix} L' & S' & J \\ m_L' & m_S' & -M \end{pmatrix} \begin{pmatrix} l_1 & l_2 & L \\ m_1 & m_2 & m_L \end{pmatrix} \begin{pmatrix} l_1' & l_2' & L \\ m_1' & m_2' & -m_L' \end{pmatrix} \\ & \times [1 - (-1)^F] \left\langle \bar{1}, \bar{2} \left| \frac{1}{r_{12}} \right| 1, 2 \right\rangle + [(-1)^{F+P} - (-1)^F] \left\langle \bar{2}, \bar{1} \left| \frac{1}{r_{12}} \right| 2, 1 \right\rangle = 0, \end{aligned} \quad (2.11)$$

where

$$E_{01,02} = -Z^2/(2n_{1,2}^2). \quad (2.12)$$

The matrix elements can be analytically expressed as

$$\begin{aligned} \left\langle \bar{1}, \bar{2} \left| \frac{1}{r_{12}} \right| 1, 2 \right\rangle &= \sum_{\lambda_1} (-)^{m'_1+m_2} [(2l_1+1)(2l_2+1)(2l'_1+1)(2l'_2+1)]^{1/2} (2a)^{l'_2} (2b)^{l_2} (2c)^{l'_1} (2d)^{l_1} \\ &\times \begin{pmatrix} l'_1 & \lambda_1 & l_1 \\ 0 & 0 & 0 \end{pmatrix} \begin{pmatrix} l'_1 & \lambda_1 & l_1 \\ -m'_1 & m'_1 - m_1 & m_1 \end{pmatrix} \begin{pmatrix} l'_2 & \lambda_1 & l_2 \\ 0 & 0 & 0 \end{pmatrix} \begin{pmatrix} l'_2 & \lambda_1 & l_2 \\ -m'_2 & m_1 - m'_1 & m_2 \end{pmatrix} \\ &\times N_{n_1 l_1} N_{n_2 l_2} N_{n'_1 l'_1} N_{n'_2 l'_2} \sum_{k_1 k_2 k_3 k_4} \frac{\alpha_{k_1} \alpha_{k_2} \alpha_{k_3} \alpha_{k_4} (2a)^{k_1} (2b)^{k_2} (2c)^{k_3} (2d)^{k_4}}{(k_1! k_2! k_3! k_4! \beta_{k_1} \beta_{k_2} \beta_{k_3} \beta_{k_4})} \\ &\times \left\{ \sum_{s=0}^{KA-\lambda_1} \frac{(KA-\lambda_1)!(KC-s)!}{(c+d)^{s+1} (KA-\lambda_1-s)!(a+b+c+d)^{KC-s+1}} \right. \\ &- \sum_{s=0}^{KA-\lambda_1+1} \frac{(KA+\lambda_1+1)!(KC-s)!}{(c+d)^{s+1} (KA+\lambda_1+1-s)!(a+b+c+d)^{KC-s+1}} \\ &\left. + \frac{(KA+\lambda_1+1)!(KC-KA-\lambda_1-1)!}{(c+d)^{KA+\lambda_1+2} (a+b)^{KC-KA-\lambda_1}} \right\}, \quad (2.13) \end{aligned}$$

where $\alpha = -n + L + 1$ and $\beta = 2l + 2$,

$$\alpha_k = \alpha(\alpha+1)\cdots(\alpha+k-1),$$

$$\beta_k = \beta(\beta+1)\cdots(\beta+k-1),$$

$$N_{nl} = \left(\frac{Z}{a_0}\right)^{3/2} \frac{2}{n^2(2l+1)!} \left\{ \frac{(n+1)!}{(n-l-1)!} \right\}^{1/2},$$

$$a = \frac{Z}{n'_2}, \quad b = \frac{Z}{n_2}, \quad C = \frac{Z}{n'_1}, \quad d = \frac{Z}{n_1},$$

$$KA = k_3 + k_4 + l_1 + l'_1 + 1,$$

$$KC = k_1 + k_2 + k_3 + k_4 + l_1 + l_2 + l'_1 + l'_2 + 3,$$

$$k_1 = n'_2 - l'_2 - 1, \quad k_2 = n_2 - l_2 - 1, \quad k_3 = n'_1 - l'_1 - 1,$$

$$k_4 = n_1 - l_1 - 1, \quad (2.14)$$

with the selection rules

- (1) $\lambda_1 = \text{maximum}\{|l'_1 - l_1|, |l'_2 - l_2|\}$ to *minimum* $\{(l'_1 + l_1), (l'_2 + l_2)\}$,
- (2) $l'_1 + l_1 + \lambda_1, l'_2 + l_2 + \lambda_1$ must be even,
- (3) $m'_1 - m_1 = -(m'_2 - m_2)$.

An evaluation of the expression $\left\langle \bar{2}, \bar{1} \left| \frac{1}{r_{12}} \right| 2, 1 \right\rangle$ then is straightforward.

About 300 energy levels have been calculated for a helium atom. The accuracy of the results was checked by means of two independent methods. First, the low excitation energy levels were calculated by the variational method. Second, we used the simple device of comparing the eigenvalues obtained from matrices of varying size. We found a satisfactory precision.

2. The spectral statistics

After unfolding the calculated spectrum⁵ the distribution function $P(s)$ for the spacing $s = X_{i+1} - X_i$ between neighboring energy levels X_{i+1} and X_i is shown in a histogram plot in Fig. 4(a). The long-range correlation of the spectrum, the rigidity $\Delta_3(l)$ is illustrated in Fig. 4(b) by dots. It turns out that the statistical fluctuation properties of a helium atom spectrum exhibit nearly a regular Poisson distribution as shown in the solid curves in Figs. 4(a)–4(d). In order to know more about the function of the repulsive Coulomb interaction between electrons in addition to the central, attractive Coulomb potential, we multiply the term $1/r_{12}$ in Eq. (2.9) by a factor f . At $f \simeq 1.6$ the calculated nearest-neighboring

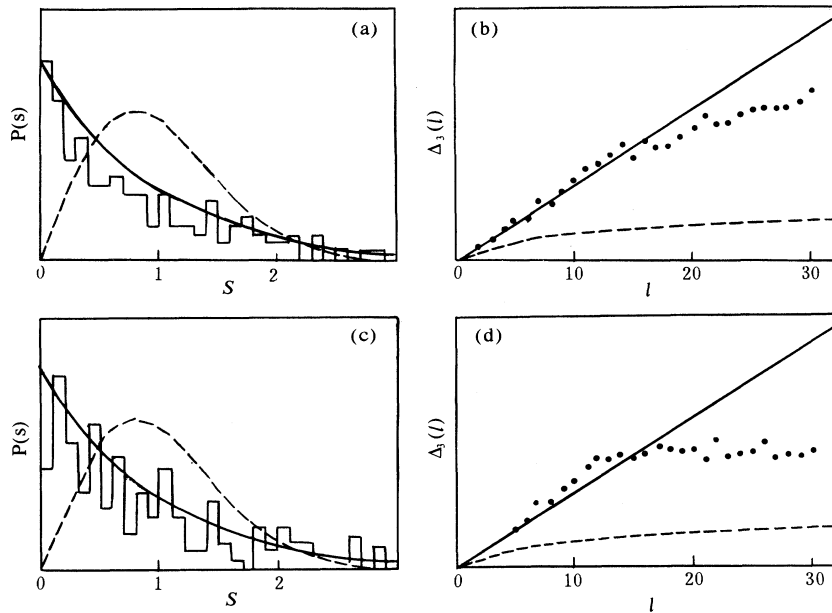


FIG. 4. The statistical fluctuation properties of the helium atom. (a) The distribution function $p(s)$ for the nearest-neighbor spacings plotted as histogram. (b) Δ_3 statistics of the spectrum shown as dots. (c), (d) $P(s)$ and Δ_3 with the condition that the electron-electron interaction is taken as f/r_{12} with $f=1.6$. In (a)–(d) solid lines give standard Poisson fluctuation distributions and dashed lines show standard GOE fluctuation distributions.

spacing distribution and $\Delta_3(l)$ are shown in Figs. 4(c) and 4(d), respectively. As indicated, the number of zero spacing levels is considerably reduced. The level spacing distribution shifts towards the larger spacings, indicating that level repulsion emerges. But still the distribution is closer to Poisson than GOE [dashed curve in Figs. 4(a)–4(c)]. The distribution of $\Delta_3(l)$ also declined somewhat toward a GOE distribution, but is still more like a Poisson distribution. At $f > 1.6$ some positive levels appear, demonstrating the dissociation of helium. So the electron-electron residual interaction is not sufficient to significantly break the dynamical symmetry of the central nuclear field, even though the interaction is amplified artificially.

The energy of each individual electron is not conserved because the interaction between electrons is given by

$$\frac{1}{r_{12}} = \frac{1}{r_>} \sum_{\lambda=0}^{\infty} \left(\frac{r_<}{r_>} \right)^{\lambda} \frac{4\pi}{2\lambda+1} \sum_{\mu=-\lambda}^{\lambda} (-1)^{\mu} Y_{\lambda\mu}(\theta_1, \varphi_1) \times Y_{\lambda-\mu}(\theta_2, \varphi_2), \quad (2.15)$$

in atomic units, where $r_<, r_>$ denote the smaller, larger of r_1, r_2 , respectively. The potential thus depends on the azimuthal angles of two electrons. Taking $f=1.6$, keeping r_1 constant and placing \vec{r}_1 in the fixed direction with $\phi = 0$ where ϕ is the angle between \vec{r}_1 and \vec{r}_2 , the equipotential lines as a function of ϕ are shown in Fig. 5. Due to the repulsive correlation effect between electrons the potential changes very steeply on the right side of the plot (corresponding to the direction of \vec{r}_1) and more gradually on the left side. But the shapes of the equipotential lines do not deviate much from circles, especially in the region of low excitation energies, indicating very mild perturbation. Here only about 300 levels have been calculated, and the high excitation energy region is not achieved. In this slightly distorted potential field in which the fluctu-

ations only declined a little from Poisson to GOE types, the KAM theorem qualitatively governs quantum system of the helium atom.

To summarize, with increasing strength of turbulence, three systems show different dynamical behavior because their equipotential lines have undergone different ways of deformation. The degree of symmetry breaking as well as the way in which symmetry is lost are different one from another.

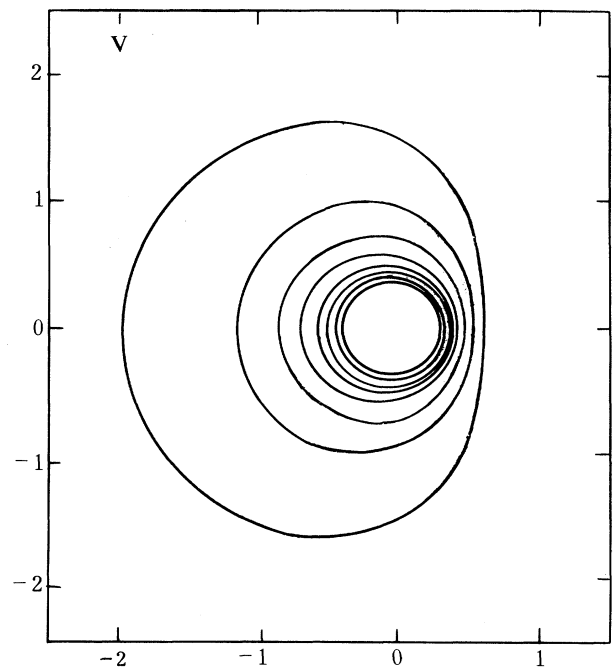


FIG. 5. The equipotential lines of the helium atom taken by varying the angle between the radial vector \vec{r}_1 of electron 1 (here the r_1 =constant, at $\phi = 0$) and \vec{r}_2 of electron 2.

III. THE STABILITY OF DYNAMICS AND THE NEGATIVE CURVATURE OF THE POTENTIAL

In the previous section the dependence of the statistical behavior on the geometrical shape of the equipotential lines was demonstrated, and the shapes of the equipotential lines were compared with those for the boundaries of the two-dimensional billiards. To estimate the effect of shapes on the dynamical behavior quantitatively, one has to estimate the rate of separation of neighboring trajectories in the phase space.

A. The analysis of stability of the classical trajectories

For a Hamiltonian

$$H(\vec{p}, \vec{r}) = p^2/2 + V(\vec{r}), \quad (3.1)$$

with the initially neighboring trajectories $\{\vec{r}_1(t), \vec{p}_1(t)\}$ and $\{\vec{r}_2(t), \vec{p}_2(t)\}$, the linearized equations of motion for the deviations

$$\vec{\xi}(t) = \vec{r}_1(t) - \vec{r}_2(t), \quad \vec{\eta}(t) = \vec{p}_1(t) - \vec{p}_2(t) \quad (3.2)$$

have the forms

$$\dot{\vec{\xi}}(t) = \vec{\eta}, \quad \dot{\vec{\eta}}(t) = -\hat{S}(t)\vec{\xi}, \quad (3.3)$$

where $\hat{S}(t)$ is the matrix constructed from the second derivatives of the potential $V(\vec{r})$, calculated along the fiducial trajectory $\vec{r}_1(t)$:

$$S_{ij}(t) = \frac{\partial^2 V}{\partial r_i \partial r_j} \Big|_{\vec{r}=\vec{r}_1(t)}. \quad (3.4)$$

The stability of the motion of the dynamical system is described in the N -dimensional case by the $2N \times 2N$ matrix

$$\hat{\Gamma} = \begin{vmatrix} \hat{0} & \hat{I} \\ -\hat{s}(t) & \hat{0} \end{vmatrix} \quad (3.5)$$

where $\hat{0}$ and \hat{I} are zero and unit $N \times N$ matrices, respectively. One can find a time-dependent transformation T such that

$$(\hat{T}\Gamma(t)\hat{T}^{-1})_{ij} = \lambda_i(t)\delta_{ij}. \quad (3.6)$$

If at least one of the eigenvalues λ_i is real, then the separation of the trajectories grows exponentially, and thus the motion is unstable. Imaginary eigenvalues correspond to stable motion. In general, the eigenvalues and therefore, the nature of the motion change with time.

To diagonalize the matrix $\hat{\Gamma}(t)$ is equivalent to solving the original equations of motion. Bolotin *et al.*⁸ assumed that the time dependent $\hat{S}(t)$ can be eliminated by replacement of the time-dependent point $\vec{r}_1(t)$ of the phase space by a time-independent coordinate \vec{r} . This reduces Eqs. (3.3) to

$$\dot{\vec{\xi}} = \vec{\eta}, \quad \dot{\vec{\eta}} = -\hat{S}(\vec{r})\vec{\xi}, \quad (3.7)$$

in which the coordinate \vec{r} is regarded as a time-

independent parameter. The problem is then greatly simplified. For a system with two degrees of freedom the equation for the eigenvalues of the matrix Γ takes the form

$$\det \begin{vmatrix} -\lambda & 0 & 1 & 0 \\ 0 & -\lambda & 0 & 1 \\ -\frac{\partial^2 V}{\partial r_1^2} & -\frac{\partial^2 V}{\partial r_1 \partial r_2} & -\lambda & 0 \\ -\frac{\partial^2 V}{\partial r_1 \partial r_2} & -\frac{\partial^2 V}{\partial r_2^2} & 0 & -\lambda \end{vmatrix}. \quad (3.8)$$

Its solution is

$$\lambda_{1,2,3,4} = \pm[-b \pm \sqrt{b^2 - 4c}]^{1/2}, \quad (3.9)$$

where

$$b = S_p \hat{S}(\vec{r}) = \frac{\partial^2 V}{\partial r_1^2} + \frac{\partial^2 V}{\partial r_2^2},$$

$$c = \det \hat{S}(\vec{r}) = \frac{\partial^2 V}{\partial r_1^2} \frac{\partial^2 V}{\partial r_2^2} - \left(\frac{\partial^2 V}{\partial r_1 \partial r_2} \right)^2. \quad (3.10)$$

If we assume $b > 0$, then under the condition that $c > 0$ the solutions λ are purely imaginary and the motion is stable. For $c < 0$, one pair of roots becomes real, and this leads to an exponential separation of neighboring trajectories. It turns out that c has the same sign as the Gaussian curvature of the potential-energy surface.

For a system with more than two degrees of freedom, which is often the case, it is rather complicated to calculate the eigenvalues. Nevertheless, we may always start by evaluating the curvature of the properly projected two-dimensional equipotential surfaces. At the potential energies where the curvatures of equipotential lines are all positive, the motion is regular. If the motion for some time sweeps across the region where the curvature of the equipotential line is negative, the motion at longer periods will ultimately lead to a chaotic type.

B. Evaluation of the stability of the dynamical behavior for given examples

(i) For the Hamiltonian of a hydrogen atom in a magnetic field, the values of c are plotted in Fig. 6 for different scaled energies $\epsilon = -0.8, -0.5, -0.4, -0.3, -0.2, -0.1$ as a function of $\tilde{\rho}$ in solid lines, and the dashed lines show equipotential lines for these corresponding ϵ 's, respectively, as functions of \tilde{z} and $\tilde{\rho}$. So the region for equipotential lines where c becomes negative is clearly found in the figure. At $\epsilon \geq -0.3$ the negative curvature appears, this leads to a chaotic behavior of the system, indicating a quantitative limit for the KAM theorem about at what amplitude the perturbation is strong enough to cause irregular motion. Again the results are consistent with the dynamical conclusion of Ref. 4. The appearance of the negative curvature depends on its scaled energy $\epsilon \equiv E\gamma^{-3/2}$. For definite ϵ , for example, for the case of $\epsilon = -0.3$, the negative curvature of the equipotential line just begins to appear. Since the energy of the hydrogen

atom E is negative, the highly excited part of the energy spectrum corresponds to smaller absolute value of E , so weaker magnetic-field strength (small γ) is needed to fulfil $\epsilon = -0.3$. On the contrary, for the lower excited part of the energy spectrum, stronger field strength (bigger γ) is needed to achieve $\epsilon = -0.3$ in order to cause chaotic motion. For different parts of the energy spectrum, GOE statistics demands different γ . Comparing Figs. 2 and 6, at $\epsilon = -0.54$, the curvature of the equipotential line is always positive, so the motion is regular. At $\epsilon = -0.12$ the negative curvature appears in the equipotential line, and the motion is chaotic.

(ii) For a system with H given by Eq. (2.6)

| k | 1 | 2 | 3 | 4 | 5 | 6 | 7 | 8 | 9 | 10 |
|-----------|----|----|----|----|-----|------|------|------|------|------|
| b/x^2 | 28 | 32 | 36 | 40 | 44 | 48 | 52 | 56 | 60 | 64 |
| c/x^2 | 96 | 96 | 72 | 24 | -48 | -144 | -264 | -408 | -576 | -768 |
| λ | Im | Im | Im | Im | Re | Re | Re | Re | Re | Re |

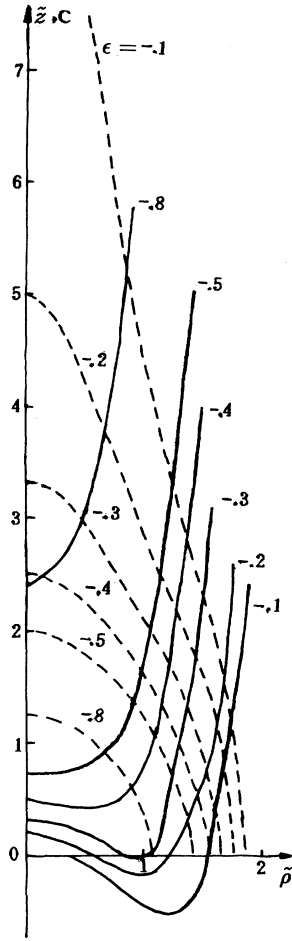


FIG. 6. The c values of the potential for a hydrogen atom in a uniform magnetic field are shown for different scaled energies $\epsilon = -0.8, -0.5, -0.4, -0.3, -0.2, -0.1$ as a function of ρ , and are plotted as solid lines. The dashed lines are the equipotential lines for corresponding ϵ values indicated in the plot.

$$V = x^4 + \frac{1}{2}y^4 + 2z^4 + ky^2(x^2 + z^2), \quad (3.11)$$

the sign of the curvature of the equipotential lines in Fig. 3 is evaluated as follows: $b = 2(6 + k)(x^2 + y^2)$, which is positive; $c = 12k(2x^4 + y^4) + 12(6 - k^2)x^2y^2$. At $K=0$, $c = 72x^2y^2$, c is positive. Then $\lambda = \pm\sqrt{-12(x^2 - y^2) \pm \sqrt{x^4 + y^4}}$ is always purely imaginary, and the motion is regular. At $k > 0$ since the negative curvature apparently would first appear at the point around the line $x^2 = y^2$, the properties of the eigenvalues of the potential are calculated at $x^2 = y^2$, and some results in the region of $x \geq 0$ and $y \geq 0$ are shown below:

where Im means that λ 's are all imaginary and Re means that at least one pair of λ 's is real. Thus, at $k \geq 5$ the sign of the curvature becomes negative and chaotic motion appears. This is in accordance with the dynamical results calculated in Ref. 6. This conclusion has no restrictions for any magnitude of potential V .

(iii) For the system of the helium atom, the information about the sign of the curvature of equipotential lines considered above is listed below as a function of energy E in atomic units at $\phi = 0$ (ϕ is the angle between radial vectors of two electrons) where the negative curvature would appear most probably:

| | | | | | |
|-----------|-------|-------|-------|-------|-------|
| E | -5 | -4 | -3 | -2.5 | -2 |
| b | 93.83 | 66.9 | 52.7 | 49.8 | 49.6 |
| c | 420.7 | 324.7 | 267.3 | 214.3 | 201.8 |
| λ | Im | Im | Im | Im | Im |

Since c is always positive, the eigenvalues λ are all imaginary. As a consequence a GOE-type statistical fluctuation has not been found for the helium atom. Again notice that b and c are all energy dependent.

IV. CONCLUSIONS

By comparing the dynamical properties of a quantum system with those of its analog of classically chaotic system, it is found that within the classical limit the quantum system manifests itself in fluctuation properties of global energy levels. The destruction of any good quantum number is responsible for the dynamical fluctuation properties. Chaotic behavior is associated with the breaking of the dynamical symmetry of the system. The dynamical symmetry can be divided into two parts: One is the geometrical symmetry of a set of equipotential lines. The appearance of the negative curvature is necessary for the instability of the motion, and the chaotic motion may start at zero curvature. To some extent this gives a quantitative measurement demanded qualita-

tively by the KAM theorem. The second part is demonstrated by the way in which the geometrical equipotential lines are distributed, which reflects the specific form of the potential. It turns out that the dynamical behavior of the system is determined by the former geometrical symmetry. The electron-electron residual interaction, in addition to the central field of the helium atom, is not strong enough to change the curvature of its equipotential lines from positive to negative, even if the interaction is amplified artificially to the greatest possible extent (short of dissociation). Therefore, the energy spectrum of the helium atom shows Poisson fluctuations. We have shown that the equipotential lines give information about the symmetry of the system, indicating the degree of symme-

try breaking, as well as the way in which the symmetry is lost.

ACKNOWLEDGMENTS

One of the authors (L.J.) wishes to gratefully acknowledge the hospitality of Professor H. A. Weidenmuller while at the Max-Planck-Institute for Nuclear Physics, Heidelberg, and discussions with Professor Weidenmuller and Professor A. Abdul Magd. This work was supported by Grant No. LWTZ-1298 of the Chinese Academy of Science.

¹ O. Bohigas and M.J. Giannoni, in *Mathematical and Computational Methods in Nuclear Physics*, edited by Dehesa J.S. *et al.*, Lecture Notes in Physics, Vol. 209 (Springer-Verlag, New York, 1984), p. 1; O. Bohigas *et al.*, in *Quantum Chaos and Statistical Nuclear Physics*, edited by T.H. Seligman *et al.*, Lecture Notes in Physics, Vol. 263 (Springer-Verlag, New York, 1986), p. 18.

² M.V. Berry, *Ann. Phys. (N.Y.)* **131**, 163 (1981). O. Bohigas, in *The Compound Nucleus: A Classically Chaotic Quantum System*, edited by J.L. Durell *et al.*, IOP Conf. Proc. No. 86

(Institute of Physics and Physical Society, London, 1986), p. 511.

³ D. Delande and J.C. Gay, *Phys. Rev. Lett.* **57**, 2006 (1986).

⁴ H. Friedrich and D. Wintgen, *Phys. Rep.* **183**, 37 (1989).

⁵ T.H. Seligman, J.J.M. Verbaarschot, and M.R. Zirnbauer, *J. Phys. A* **18**, 2751 (1985).

⁶ T.H. Seligman, J.J.M. Verbaarschot, and M.R. Zirnbauer, *J. Phys. A* **18**, 2227 (1985).

⁷ J. Reichl and H. Buttner, *Europhys. Lett.* **4**, 1343 (1987).

⁸ Yu.L. Bolotin *et al.*, *Sov. J. Part. Nucl.* **20**, 372 (1989).